Geothermics 100 (2022) 102349

Contents lists available at ScienceDirect

Geothermics

journal homepage: www.elsevier.com/locate/geothermics

Hydrochemical and biotic control on iron incrustations in groundwater heat pump systems: Case study from a saline, anoxic aquifer in Melhus, Norway

Lars A. Stenvik[a,*], Sondre Gjengedal[b], Randi K. Ramstad[a,c], Bjørn S. Frengstad[a]

[a] Norwegian University of Science and Technology, S. P. Andersens vei 15A, Trondheim N-7491, Norway
[b] Norwegian Geotechnical Institute, P.O. Box 5687 Torgarden, Trondheim N-7485, Norway
[c] Asplan Viak AS, Hotellgata 2, Stjørdal N-7500, Norway

ARTICLE INFO

Keywords:
Groundwater heat pump
Incrustation
Iron oxide
Iron sulfide
Clogging
Iron-oxidizing bacteria

ABSTRACT

Clogging by incrustations of nine groundwater heat pump (GWHP) systems in Melhus, Norway have been investigated by field and laboratory methods for water quality and incrustation composition. Iron oxides incrust systems extracting relatively shallow, low-saline groundwater, while iron sulfides are associated with deeper, more saline groundwater. Hydrochemical conditions in iron oxide clogged GWHP systems are favorable for the growth of iron-oxidizing bacteria. Also, sediment deposits clog the well systems. The variety of incrustation problems detected in Melhus emphasizes that clogging must be expected and dealt with, instead of solely attempted avoided through system design or re-location.

1. Introduction

Shallow aquifers function as storages for solar heat. This can be utilized for heating and cooling of buildings by means of a groundwater heat pump (GWHP) system. An aquifer thermal energy storage (ATES) system additionally comprises seasonal storage and extraction of excess building heat to/from the aquifer. Both these open-loop ground source heat pump systems essentially comprise two groundwater wells, one for extraction and one for injection. The extracted groundwater undergoes heat exchange to/from a heat pump coupled to a building heat distribution system before injection. The technologies reduce the electricity demand compared to conventional electrical heating. However, their operation is impeded by dissolved and suspended material of inorganic and/or organic origin in the groundwater which may precipitate or deposit to form incrustations. Incrustations have been observed to clog vital parts of GWHP and ATES systems such as well screens and filters, pumps, pipes and heat exchangers (Bakema, 2001; Eggen and Vangsnes, 2005; Lerm et al., 2011; Possemiers et al., 2016; Burté et al., 2019; Gjengedal et al., 2020). Clogging impels costly rehabilitations or even reconstructions, with the remedy depending on incrustation type and extent (Mansuy, 1998; Bakema, 2001; Houben and Treskatis, 2007). This underlines the importance of properly identifying and characterizing incrustations in GWHP and ATES systems in time.

This article presents water chemical and incrustation investigations of nine GWHP systems in Melhus, Norway which have experienced clogging, and aims to unravel incrustation composition and genesis.

1.1. Incrustations in groundwater wells

Incrustations are categorized as either chemical, biotic or mechanical, but the processes are often concomitant. The most common chemical incrustations in groundwater wells are iron oxides/hydroxides (both termed iron oxides in this article) (Houben and Treskatis, 2007). Iron oxides form when dissolved oxygen (O_2) oxidizes dissolved ferrous iron (Fe^{2+}) to practically insoluble ferric iron (Fe^{3+}) which precipitates as solid iron oxide ($Fe(OH)_3(s)$). The reaction proceeds according to (Stumm and Morgan, 1996):

$$4Fe^{2+} + O_2 + 10H_2O = 4Fe(OH)_3(s) + 8H^+ \quad (1)$$

Oxidation of ferrous iron is the rate-controlling step of the iron oxide

Abbreviations: BART, Biological activity reaction test; GWHP, Groundwater heat pump; ICP-MS, Inductively coupled plasma mass spectrometry; IOB, Iron-oxidizing bacteria; LOI, Loss on ignition, weight-loss of incrustation samples ignited at 400 °C; Q, Volumetric groundwater pumping rate; SLYM, Slime-forming bacteria; SRB, Suflate-reducing bacteria; XRD, X-ray diffraction.

* Corresponding author.
E-mail address: lars.a.stenvik@ntnu.no (L.A. Stenvik).

https://doi.org/10.1016/j.geothermics.2022.102349
Received 25 October 2021; Received in revised form 20 December 2021; Accepted 8 January 2022
Available online 16 January 2022

precipitation at circumneutral pH. The homogenous (i.e., in the water phase) kinetic rate of iron oxidation can be described by the equation (Stumm and Lee, 1961)

$$-\frac{d[Fe^{2+}]}{dt} = k\left[Fe^{2+}\right][O_2][H^+]^{-2} \quad (2)$$

where k is the homogenous rate constant and parentheses indicate concentrations. The rate constant k generally decreases with increasing ionic strength, but an exact value is difficult to determine since numerous hydrochemical parameters inhibit or catalyze the reaction Sung and Morgan, 1980). It is evident from Eq. (1) and ((2) that higher pH and oxygen concentrations accelerate iron oxidation. Typically, there is a vertical zonation of redox environments in soils, with oxic conditions close to the surface which gradually become more anoxic with depth as oxygen is depleted through redox reactions. In anoxic environments, iron is found as reduced and dissolved Fe^{2+} ions. Production wells may extract water from different redox zones, causing them to mix and trigger ferrous iron oxidation by oxygen (van Beek, 1989). Furthermore, oxygen in-leakage through improperly sealed parts of the groundwater pipeline also poses risk of iron-oxygen reactions (Bakema, 2001). The amorphous, unstable ferrihydrite ($Fe(OH)_3$) that usually first forms will recrystallize to the more stable goethite (FeOOH) with time. Manganese oxides can also incrust well systems but are less frequent than iron oxides. This is due to manganese's lower earth crust abundance, higher oxygen demands for oxidation and slower reaction kinetics (Stumm and Morgan, 1996; Houben and Treskatis, 2007).

Eq. (2) does not consider the effect of heterogenous iron oxidation which occurs on surfaces. The presence of oxidized iron (Fe^{3+}) on solid surfaces will sorb dissolved ferrous iron and catalyze oxidation. This causes an autocatalytic effect, described by the combined homogenous and heterogenous rate equation (Tamura et al., 1976)

$$-\frac{d[Fe^{2+}]}{dt} = \left(k[O_2][H^+]^{-2} + k'K[O_2][H^+]^{-1}\left[Fe^{3+}\right]\right)\left[Fe^{2+}\right] \quad (3)$$

where k' is the heterogenous rate constant, K is the adsorption constant for ferrous iron onto iron oxides. The heterogenous reaction's first order dependence on pH compared with the second order dependence of homogenous oxidation, suggest that the heterogenous effect is most pronounced at lower pH levels. Iron-oxidizing bacteria (IOB) which gain energy from iron oxidation (e.g., Gallionella and Leptothrix) thrive on solid surfaces and may further catalyze iron oxidation. Different genera have different hydrochemical preferences, for instance with regards to dissolved oxygen and iron concentrations, pH, and salinity Houben and Treskatis, 2007; McBeth et al., 2013; Eggerichs et al., 2014). Thus, the apparent increase in iron oxidation with pH and oxygen from Eq. (2) and ((3) may be disturbed indirectly by hydrochemical conditions which dictate the IOB genera's growth conditions and influence on the rate constant k'.

Oxygen depleted, iron-rich conditions facilitate iron sulfide mackinawite (FeS) and/or iron carbonate siderite ($FeCO_3$) incrustations, if dissolved sulfur and/or carbonate are present, respectively. Reducing, sulfur-rich environments are characterized by the smell of rotten eggs (i.e., H_2S gas). Sulfide precipitation is accelerated by the presence of sulfate-reducing bacteria (SRB), which nurture from sulfate (SO_4^{2-}) reduction (Houben and Treskatis, 2007). SRB also facilitate corrosion of metallic iron, together with high oxygen contents, low pH, and high salinity. Corrosion will also produce iron oxides (rust) and sulfide incrustations. Rust possesses magnetic properties, unlike iron oxides of non-corrosion origin (Houben and Treskatis, 2007).

Biotic incrustations, or biofouling, are caused by microorganisms and other biotic material building up fluffy and slimy biofilms. The group of microorganisms responsible for the formation of biofilms are therefore often termed slime-forming bacteria (SLYM). Their build-up around production and injection wells is facilitated by the constant nutrient supply from locally elevated groundwater flow rates. The SLYM and IOB bacteria categories partly overlap. Thus, biofouling and iron oxides incrustations are commonly found in the same wells (Mansuy, 1998).

Mechanical incrustations comprise aquifer or well filter pack materials which have entered and deposited in the well system. This is typically caused by improper well screen and/or filter design or development, or too high inflow velocities in and around the well screen (Bakema, 2001). The latter could be triggered, for example, by iron oxide incrustations gradually decreasing the available inflow cross-section (Mansuy, 1998).

1.2. Study area

Nine GWHP systems have been established in the town center of Melhus, Mid-Norway in the period 1999–2015, see Fig. 1. The GWHP systems supply heating and cooling to the 6,686 inhabitants' (Statistics Norway, 2020) apartments, nursing homes, schools, grocery stores and offices, by extracting water from the same aquifer. The Melhus aquifer consists of coarse unconsolidated glaciofluvial sediments hydraulically connected to the river Gaula (Hellestveit, 2018), and covered by a marine clay layer. The aquifer has both unconfined and confined characteristics, depending on location, due to inclination and variable thickness of the marine clay layer. The natural groundwater table is located ~10–20 m below ground level. The area's marine history with isostatic uplift in Holocene (Reite, 1990) has left the aquifer with a salinized groundwater quality, with salinity increasing with the thickness of the overlying clay layer (Brøste, 2017).

All GWHP systems in Melhus comprise a production well with a submersible pump installed above the well screen. The pumped water is then led to a heat exchanger, where the ~6–8 °C groundwater temperature is reduced/increased ~3 °C. Then, the water is either re-infiltrated to the aquifer through an injection well (6 out of 9 systems) or lead to the local sewage system (3 out of 9 systems), see Fig. 1. All well filters are naturally developed (i.e., not gravel packed), and with continuously slotted well screens. Seven systems operate at a constant groundwater pumping rate, while two operate with variable speed drive according to the heat demand, see Fig. 1. The pumping rates range between 4 and 17 l/s (Gjengedal et al., 2020), see Table 1.

Previous investigations have revealed incrustation problems in all nine GWHP systems. The first incrustation review by Riise (2015) suggested iron oxides as the main incrustation problem. The problems have been further studied in the national research projects ORMEL and ORMEL 2 ("Optimal utilization of heating and cooling in Melhus (and Elverum)") (Brøste, 2017; Gjengedal et al., 2018, 2019, 2020). The water chemistry, incrustation mineralogy and camera inspections of wells have been studied previously (Riise 2015; Brøste, 2017; Gjengedal et al., 2018). However, new hydrochemical measurements have been deemed necessary since the former ones did not include air-tight flow-through cell measurements of parameters such as pH, dissolved oxygen and redox potentials. Supplemental analysis of incrustation mineralogy, microbiology and camera inspections were also considered favorable to assess the link between water quality and incrustation genesis.

2. Methods

2.1. Water quality

The water chemistry was investigated by a combination of laboratory analysis of water samples and field measurements between May 2019-June 2021. Each GWHP was sampled and measured up to eight times from taps located right before and after the heat exchangers, see Fig. 1. The Oterholmgården GWHP was only sampled once due to lack of water sampling tap until spring 2021. The water chemistry of the abandoned production well at Lenavegen 3 was also investigated while performing biological activity reaction tests (see description below). Water samples

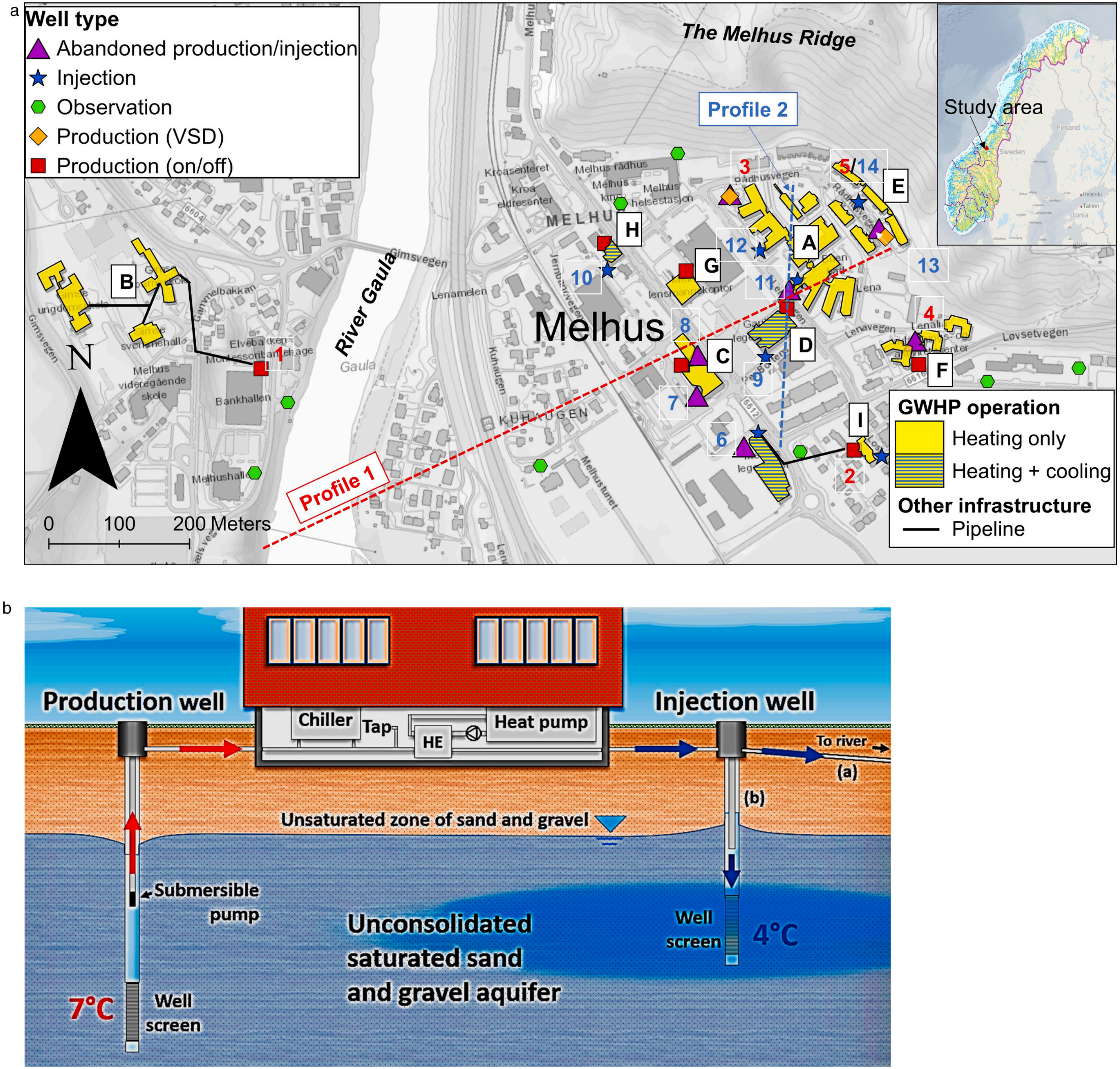

Fig. 1.. Top: Map of study area. Location of GWHP systems that re-inject groundwater (A, C, D, E, H, I) and discharge groundwater to the river Gaula (B, F, G) in the town center of Melhus is indicated. Name of systems (A-I) are given in Table 1. Profile 1 (production well 1–5) and 2 (injection wells 6–14) are presented in Fig. 5. VSD = pump operates with variable speed drive. On/off = pump operates at one single speed. Bottom: Groundwater heat pump (GWHP) system design in Melhus, Norway. Two designs exist with (a) discharge to river and (b) infiltration through an injection well (Gjengedal et al., 2019).

Table 1.
Basic information about the GWHP systems in Melhus, see Fig. 1. Q = groundwater pumping rate. bgl = below ground level. Pumping rate data is partly retrieved from Riise (2015).

	GWHP system(Start of operation)	Production well screen (meters bgl)	Q(l/s)	Injection well(s)	Clogging measures[c] (#) Rehabilitations	Reconstructions
A)	Buen (2013-)	36–44 (29.5–32.5[a])	8–9[b]	2	1	2
B)	Gimse (2009-)	19–34	6–7	–	2	0
C)	Høvdingen (2015–2020)	66–69 (65–68[a])	7.5	2	0	2
D)	Idegården (2008-)	46–60	6.5	1	2	0
E)	Lena terrasse (2003–2006, 2015-)	30–36 (27–37[a])	7–12[b]	1	8	3
F)	Lenavegen 3 (1999–2013, 2014-)	39.5–43 (17.5–23.5[a])	15–16	–	0	2
G)	Melhuset (1999-)	24.5–34.5	4	–	1	0
H)	Oterholmgården (2010-)	36–38	5.5	1	2	0
I)	Thoragården (2013-)	73–78 (79.5–83[a])	4–5	2	0	1

(a) Defect/replaced production wells. bgl = below ground level.
(b) Variable speed drive (VSD) groundwater pump.
(c) Clogging measures in wells, heat exchangers or submersible pumps per September (2021).

were filtered with a 0.45 μm membrane filter in the field and conserved with 0.1 M HNO_3 acid. All sample batches were analyzed by inductively coupled plasma mass spectrometry (ICP-MS) (Element 2 - ICP-HR-MS, ICP-MS Agilent 8800) at the Department of Chemistry, NTNU. The ICP-MS instruments could detect chloride (Cl^-) and sulfur (S). The latter could be recalculated as sulfate (SO_4^{2-}), assuming sulfate was the prevailing sulfur species . Earlier investigations have revealed low nitrate concentrations (NO_3^-) (Brøste, 2017). Therefore, ion chromatography analyses of anions were left out of this study. Only analyzes displaying charge balance $\leq \pm 5\%$ between major cations and anions were included in this study to exclude analytical errors.

Alkalinity, pH, electrical conductivity (EC), oxidation–reduction potential (ORP), dissolved oxygen (DO) and temperature were measured in situ. Alkalinity was measured by "Gran titration" (Stumm and Morgan, 1996) with Merck MColortest, while temperature, pH (WTW Sensolyt 900-P), EC (WTW TetraCon 925/C), ORP (Sensolyt ORP 900-P) and DO (WTW FDO 925) were measured by electrodes connected to a WTW Multi 3630 IDS digital meter. The ORP values were later converted to the redox potential with respect to the normal hydrogen electrode (Eh). The electrodes were submerged in a custom-made flow-through cell, to which water was lead from the same taps where water samples were taken, at 0.1–0.2 l/s flow rate. The sensors were continuously measuring every 30 s for as long as two hours, due to sluggish Eh stabilization.

Biological activity reaction tests (BART) (Hach) were used to identify microbiological activity in the GWHP systems. Tests for iron-oxidizing bacteria (IOB), sulfate-reducing bacteria (SRB) and slime-forming bacteria (SLYM) were carried out for all GWHP systems except Oterholmgården during continuous pumping. Furthermore, the Idegården, Lena terrasse and Oterholmgården GWHP and the old, abandoned production well at Lenavegen 3 were BART sampled after shut-off periods ranging from 2 h to 5 years. Longer shut-off periods are expected to increase the number of bacteria present in the water-phase (Cullimore, 2008). Thus, the BART samples taken after 2 hour and 5 years were not necessarily comparable. The BART test procedure comprised of adding water sampled from the GWHP system/well to an incubator in the laboratory. Type and semi-quantitative count of bacteria couldbe determined based on time until and type of reaction in the BART incubators.

2.2. Laboratory incrustation analysis

Thirteen incrustation samples were brought to the laboratory for x-ray diffraction (XRD), ICP-MS, loss on ignition (LOI) and magnetic analyses, see Table 2. XRD on single grains and bulk samples and ICP-MS of dissolved incrustations were used to analyze mineralogical and chemical composition, respectively. LOI was used to assess the incrustations' organic content. Observing the incrustation materials' attraction to a magnet was used assess the presence of magnetic minerals (e.g., metallic iron). Houben and Treskatis (2007) recommend sampling fresh incrustation material to avoid maturation and contamination. It was difficult to obtain fresh samples from the GWHP systems. Consequently, incrustations which had been stored up to five years under atmospheric conditions prior to sampling were included in the sampling program.

Table 2.
Summary of laboratory and field incrustation analyses in the Melhus GWHP systems. Abbreviations: HE = heat exchanger, pipe = abandoned pipe, pipe filter = filter in groundwater pipes right before heat exchanger, cell = deposits in flow-through cell after water chemical field measurements, inj. = from injection well during rehabilitation.

No.	GWHP system	Sampling site (year)	Sample appearance	Analyses* XRD	ICP-MS	LOI
1	Buen	Pipe filter (2019)	Black, hard	+	+	+
2	Gimse	Pipe (2020)[a]	Orange, brittle	+	+	+
3	Høvdingen	Pipe filter (2019)	Orange, brittle	+[b]	+	+
4	Idegården	Pipe filter (2020)	Black, hard, magnetic	+	N/A	+[c]
5	Lena terrasse	HE (2018)	Orange, gray, brittle	+	+	+
6	Lena terrasse	HE (2019)	Orange (rinsing fluid)	N/A	+	N/A
7	Lena terrasse	Inj. (2020)	Sediments, orange	+[b]	+	+
8	Lena terrasse	HE (2021)	Orange (rinsing fluid)	N/A	+	N/A
9	Lenavegen 3 (old)[d]	Pipe (2017)[a]	Rusty red, brittle	+[e]	+	+
10	Lenavegen 3 (new)[d]	Cell (2020)	Sand, gravel	+	N/A	+
11	Melhuset	Pipe (2019)[a]	Orange, layered	+	+	+
12	Oterholmgården	HE (2021)	Light yellow (rinsing fluid)	N/A	+	N/A
13	Thoragården	Cell (2020)	Black, flaky, magnetic	+[b]	+	N/A

*XRD, LOI and ICP-MS of used rinsing fluids were carried out continuously (i.e., shortly after sampling), while ICP-MS analysis of nitric acid dissolved incrustations were carried out in May 2020.
(a) Two (Gimse, Lenavegen 3) and five (Melhuset) years storage under atmospheric conditions prior to sampling.
(b) XRD analysis of single grain.
(c) Ignited at 450°C (all others at 400°C).
(d) Samples from old, abandoned production well and new, currently operating GWHP system.
(e) Data from Brøste (2017).

The samples analyzed by XRD (Bruker D8 Advance) and for LOI (Nabertherm B180) were mortared and dried at 35/65°C (XRD) and

105°C (LOI) prior to analysis. The LOI, measured as % weight loss after 4 h of ignition at 400°C, was assumed to equal the incrustation sample's organic content, as suggested by McLaughlan (1992). This temperature is conservative compared with the custom 550°C, but reduces the risk of igniting carbonates. ICP-MS analyses were performed both on (1) solid incrustations dissolved in nitric acid (HNO_3) and filtered in the mineralogy lab at the Department of Geoscience and Petroleum, NTNU (Perkin Elmer ELAN DRC II), and (2) rinsing fluid samples containing both dissolved incrustations and rehabilitation chemicals in the chemistry lab at the Department of Chemistry, NTNU (Element 2 - ICP-HR-MS, Agilent 8800). All other analyses were carried out in the mineralogical lab at the Department of Geoscience and Petroleum, NTNU.

2.3. Camera inspection and other field observations

Well camera inspections have been carried out in eight out of nine GWHP system in Melhus, see Table 1, to assess incrustation type and extent, and evaluate well rehabilitation success. The inspections were carried out from 2013 onwards by local water and wastewater entrepreneur Gjøvaag AS. Some of the inspections have already been described by Riise (2015) and Gjengedal et al. (2018; 2020).

Field observations of water quality were performed, including observation of suspended solid deposition in the flow-through cell and H_2S gas odor. Furthermore, mud color registered during drilling of the observation wells, see Fig. 1, was used to assess redox conditions. The depth where the color changed from orange/red to clear/gray was interpreted as the transition depth from oxic to anoxic iron conditions. This was based on the characteristic rusty color of iron oxides which forms under oxic conditions.

3. Results

3.1. Water quality

The GWHP systems' key hydrochemical data are summarized in Table 3. The coexistence of different water types in the Melhus aquifer is evident from the range of total dissolved solids. Most GWHP systems extract a typical seawater Na-Cl water quality, while a mixed $Ca\text{-}HCO_3$/Cl water type is found at Gimse and Lena terrasse. The groundwater is neutral-basic and alkaline. Dissolved oxygen, iron and manganese concentrations correspond to an anoxic, iron-reducing redox regime, while measured redox potentials (Eh) indicate iron oxidation as the dominant redox process (Stumm and Morgan, 1996).

None of the BART tests from the first batch (i.e., taken after longer periods of continuous pumping of the GWHP system) had reacted after 9 days in the incubator. This indicated "non-aggressive" activity of IOB, SRB and SLYM. For the second batch of BART testers (i.e., taken after pump shut-off periods), the Lenavegen 3 (abandoned production well), Lena terrasse and Oterholmgården IOB incubators yielded brown clouds and rings after 3–8 days. This indicated "moderate" (5–8 days to reaction) to "aggressive" (0–4 days to reaction) bacteria activities, see Fig. 2. "Non-aggressive" IOB activity ($\geq$ 9 days to reaction) was detected at Idegården even after pump shut-off. Some of the IOB samples reacted to form bubbles and blackened liquids. This is indicative of anaerobic and SLYM bacteria (Cullimore, 2008), respectively. The long reaction times of the SLYM and SRB incubators imply "non-aggressive" growth of these bacteria groups, see Fig. 2.

3.2. Laboratory incrustation analysis

The laboratory incrustation analyzes are summarized in Fig. 3. Goethite (FeOOH), mackinawite (FeS), quartz (SiO_2) and other silicates were the main phases detected during XRD analysis. However, the XRD analysis only yielded information about the crystalline part of the incrustation samples, which was generally low. Iron was the main element detected during ICP-MS of dissolved incrustations, with smaller amounts of calcium, sodium, and sulfur. The iron oxide dominated incrustations' ferrihydrite ($Fe(OH)_3$) weight percentages were estimated from the incrustations' iron concentration (from ICP-MS). The calculations assumed that all dissolved iron stemmed from ferrihydrite. Iron sulfide weight percentage was not estimated for the sulfide dominated Buen incrustation sample, since the nitric acid was ineffective dissolving this sample. The incrustations which contained iron oxides displayed a higher loss on ignition than those primarily consisting of iron sulfides and/or silicates. Most incrustation samples displayed a low degree of magnetism. The exceptions were the Thoragården and Idegården

Table 3.
Summary of key water chemical parameters measured in the GWHP systems, represented as mean ± two standard deviations (SD). See Table 1 for explanation for GWHP system abbreviations.

GWHP	Water samples (ICP-MS)					Field measurements				
	Fe^{2+} (mg/l)	Mn^{2+} (mg/l)	Ca^{2+} (mg/l)	Cl^- (mg/l)	SO_4^{2-} (mg/l)	TDS (g/l)	Alk (mM)	pH	Eh (mV)	DO (mg/l)
A) Buen	4.03 ± 1.97	0.63 ± 0.06	99 ± 9	552 ± 81	176 ± 19	1.53 ± 0.12	4.9 ± 0.2	7.46 ± 0.07	42 ± 28	0.03 ± 0.01
B) Gim.	1.70 ± 0.73	0.17 ± 0.02	87 ± 9	17 ± 4	130 ± 17	0.50 ± 0.05	3.5 ± 0.6	7.40 ± 0.21	47 ± 58	0.04 ± 0.00
C) Høv.	0.21 (0.14-1.01)[a]	0.07 ± 0.02	47 ± 5	998 ± 147	203 ± 22	2.24 ± 0.18	4.5 ± 0.2	8.13 ± 0.12	75 ± 48	0.7 (0.3–2.4)[a]
D) Ide.	3.97 ± 1.00	0.61 ± 0.06	107 ± 16	556 ± 103	180 ± 24	1.56 ± 0.15	5.0 ± 0.5	7.47 ± 0.05	40 ± 41	0.03 (0.03–0.19)[a]
E) Len.t.	3.49 ± 0.63	0.60 ± 0.09	138 ± 14	301 ± 64	201 ± 25	1.20 ± 0.12	5.4 ± 0.4	7.31 ± 0.11	107 ± 33	0.04 ± 0.01
F1) Len. 3 (old)	5.20 ± 0.21	0.58 ± 0.02	119 ± 5	246 ± 32	170 ± 10	1.24 ± 0.05	7.8 ± 0.5	7.13 ± 0.02	49 ± 65	0.03 ± 0.01
F2) Len. 3 (new)	4.18 ± 1.99	0.52 ± 0.05	69 ± 5	610 ± 142	139 ± 16	1.55 ± 0.22	4.5 ± 0.2	7.45 ± 0.09	8 ± 29	0.03 ± 0.01
G) Mel.	1.32 ± 0.47	0.27 ± 0.04	51 ± 8	378 ± 77	115 ± 21	1.10 ± 0.16	4.0 ± 0.3	7.92 ± 0.12	11 ± 10	0.03 ± 0.00
H) Oter.	2.31 ± 0.10	0.37 ± 0.01	52 ± 1	326 ± 11	85 ± 2	1.00 ± 0.02	4.3 ± 0.1	7.71 ± 0.02	15 ± 41	0.04 ± 0.01
I) Thor.	0.28 ± 0.07	0.05 ± 0.01	49 ± 3	948 ± 137	206 ± 24	2.21 ± 0.19	5.0 ± 0.3	8.11 ± 0.14	−19 ± 37	0.03 ± 0.00

GWHP system (number of samplings): A ($n = 8$), B ($n = 5$ water samples (ws) + alkalinity (alk), $n = 6$ for other field measurements (fm)), C ($n = 4$ ws + alk, $n = 3$ fm), D ($n = 8$), E ($n = 7$ ws + alk, $n = 8$ fm), F1 ($n = 1$), F2 ($n = 6$ ws + alk, $n = 7$ fm), G ($n = 8$), H ($n = 1$), I ($n = 7$ ws + alk, $n = 8$ fm). Where $n = 1$, analytical mean and error is displayed.

[(a)] Measured values vary considerably, thus median and range of values is displayed instead of mean±2SD.

GWHP	Lenavegen 3 (old)				Idegården		Lena terrasse		Oterholmgården	
Date(s)	03.09.20				02.12.20		02.12.20	22.01.21	17.03.21	
Shut-off period	5 years				2 hours		2 hours	2 days	1 day	
Q (l/s)	1.0				6.5		8.1	12.1	5.5	
Sampling time (min)	10	60	120	240	2	90	10	120	30	120
IOB rx. time (days)	3	4	5	5	-	-	5	7	6	6
BART-IOB incubator *(time after sampling)*	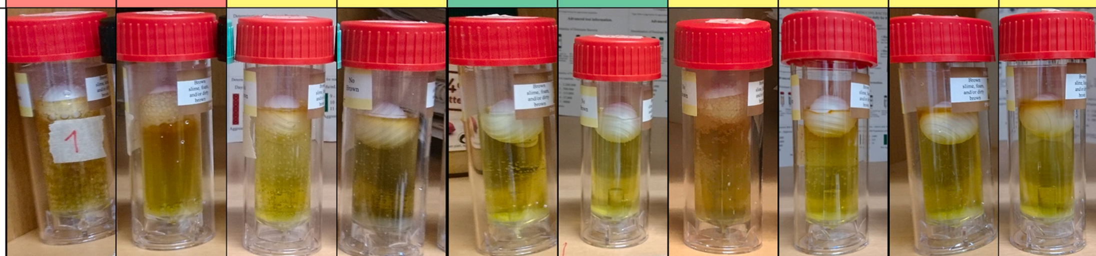									
	3 days	*4 days*	*5 days*	*5 days*	*9 days*	*9 days*	*5 days*	*7 days*	*6 days*	*6 days*
SLYM rx. time (days)	7	7	7	7	-	-	7	9	8	8
SRB rx. time (days)	-	-	-	-	-	-	N/A	-	-	-

Fig. 2.. Results from biological activity reaction tests (BART) taken after pump shut-off periods. Sampling time refers to time after re-start of pumping. Old = abandoned, defect production well, see Fig. 1. Rx. = reaction. "-" means reaction after > 9 days. Color refers to bacteria activity: red = aggressive, yellow = moderate, green = non-aggressive. N/A = not sampled.

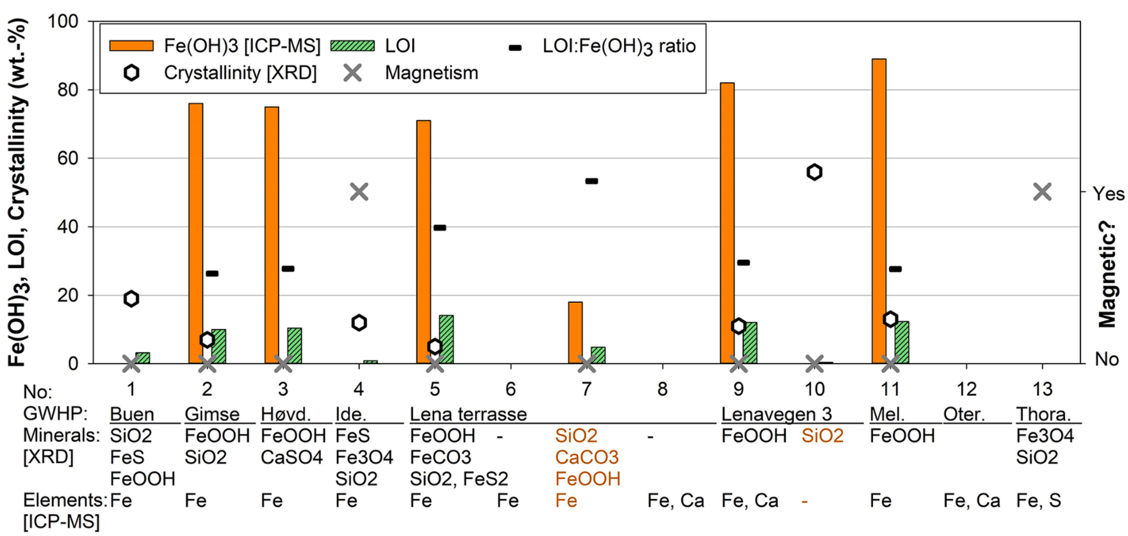

Fig. 3.. Summary of incrustation analyses. Plot of weight-percentage (wt.-%) of $Fe(OH)_3$ (calculated from ICP-MS analysis), loss on ignition (LOI) and crystallinity (from XRD analysis). Also calculated LOI: $Fe(OH)_3$ ratio and magnetism (yes/no) is plotted. "Elements [ICP-MS]" refer to elements with weight concentration ≥ 2%. XRD analyzed samples not displaying crystallinity (3, 7, 13) were performed on single grains (small sample). Mineral and element formulas: SiO2 = quartz (refers to quartz and other silicate minerals), FeS = mackinawite, FeOOH = goethite, CaSO4 = gypsum, NaCl = halite, Fe3O4 = magnetite, FeCO3 = siderite, FeS2 = pyrite, CaCO3 = calcite, Fe = iron, Ca = calcium, *S* = sulfur.

incrustations, which contained the magnetic mineral magnetite (Fe_3O_4) (from XRD).

3.3. Camera inspection and other field observations

Observations from camera inspections and drilling logs are shown in Fig. 4 and plotted versus location in Fig. 5, where observations are simplified to one single point representative for each incrustation type.

Camera inspection and laboratory incrustation analyses pointed to iron oxides and iron sulfides as the main chemical incrustation minerals. Observations during camera inspections were interpreted based on laboratory incrustations analyzes (XRD, ICP-MS) and the authors' experience with incrustation appearance (color, structure). Orange incrustations were interpreted as iron oxides. Black, hard incrustations were interpreted as iron sulfide incrustations. The latter were first wrongly interpreted as manganese oxides due to their similar visual appearance. Followingly, it could be distinguished that Gimse, Høvdingen, Lena terrasse, Lenavegen 3 (abandoned well), Melhuset and Oterholmgården suffered from iron oxide incrustations, while Buen, Idegården and Thoragården suffered from iron sulfides. Both iron oxide

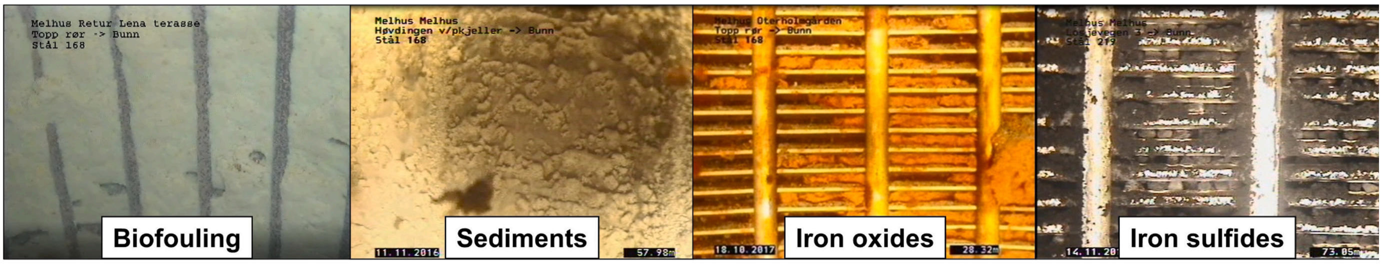

Fig. 4.. Photos from camera inspections: Lena terrasse's injection well screen in 2018 (left), Høvdingen's injection well screen in 2016 (middle left), Oterholmgården's injection well screen in 2017 (middle right), and the production well screen at Thoragården in 2016 (right).

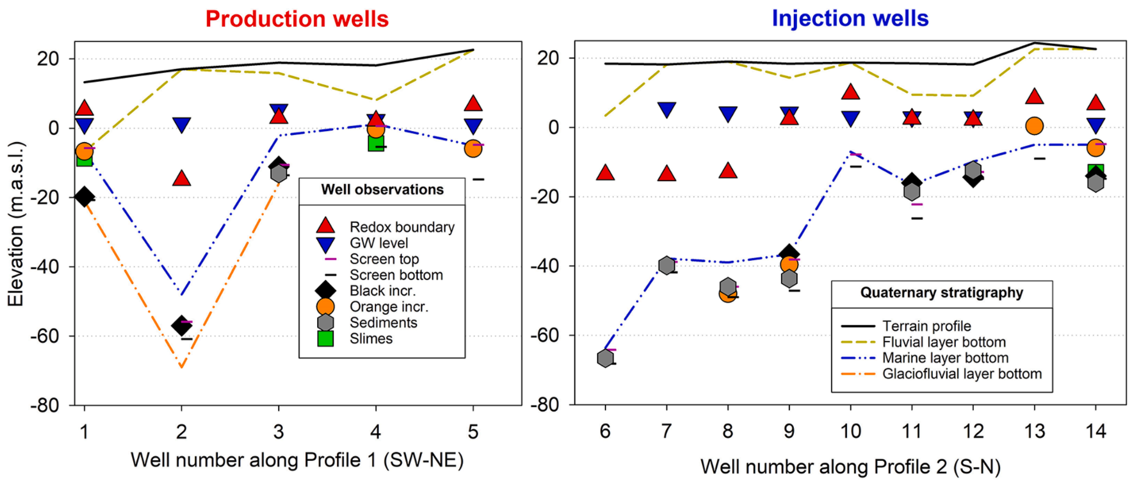

Fig. 5.. Camera inspections and drilling logs. Observations during camera inspections of production (left) and injection wells (right). X-axis not to scale. "Redox boundary" refers to transition from oxic to iron-reducing conditions, and is interpreted from visual observations during well drilling. GW = groundwater. The glaciofluvial layer bottom could not be indicated entirely along the profiles since drilling was often stopped before reaching bottom of the layer.

and sulfide incrustations were accompanied with varying levels of sediments (silicates), most likely stemming from the aquifer formation or well filter pack (i.e., mechanical incrustation). The new Lenavegen 3 GWHP production well has not been camera inspected, but deposition of gravel sized (> 2 mm) sediments in the flow-through cell have been observed several times during hydrochemical measurements.

4. Discussion

Kinetic calculations show that the water residence times (on the scale of minutes) of GWHP systems incrusted by iron oxides are well below the homogenous iron oxidation half-times (on the scale of hours to days). Half-times were calculated by modifying Eq. (2), and assuming a rate constant k around 1.4×10^{-12} mol/min (Houben, 2004). The discrepancies between reaction half- and residence time indicate that abiotic, homogenous iron oxidation is not intense enough to clog the systems alone. Severe iron oxide clogging has been detected under similar redox conditions as in the Melhus aquifer, in water supply wells in Belgrade, Serbia (Barbič et al., 1974; Dimkić et al., 2012) and an ATES system in Berlin, Germany (Lerm et al., 2011; Eggerichs et al., 2014). The activity of iron-oxidizing bacteria was identified to control the clogging at the latter two sites (Barbič et al., 1974; Lerm et al., 2011). These results suggest heterogenous, biotic catalysis should be considered for the GWHP systems in Melhus as well.

Microbes prefer to inhabit solid surfaces if nutrients are continuously supplied (e.g., around a production well screen during continuous pumping), but will start to move out in the liquid phase under more stagnant conditions (Cullimore, 2008). Thus, BART samples taken during continuous pumping is likely to reflect the background microbiological activity in the aquifer, while samples after pump shut-off periods probably reflect microbes in and around the well screen incrustations. Iron-oxidizing bacteria (IOB) and slime-forming bacteria (SLYM) incubators taken after pump shut-off periods reacted much faster than the ones taken during continuous pumping in iron oxide incrusted systems (Lena terrasse, Lenavegen 3 (old), Oterholmgården), while long reaction times were observed in the iron sulfide incrusted system (Idegården), see Fig. 2. This implies good growth conditions for IOB and SLYM bacteria in iron oxide incrusted GWHP systems.

There also seems to be a link between chemical incrustation type and hydrochemistry, see Fig. 6. Most strikingly, iron oxides seem to incrust systems extracting water of lower salinity (TDS). On the other hand, there is no distinct relation between concentration of the redox sensitive species dissolved oxygen, nitrate (Riise, 2015; Brøste, 2017; Solberg et al., 2014), iron, manganese and sulfate, and incrustation type. One exception is the Høvdingen GWHP system which measured considerably higher dissolved oxygen levels than the other systems, probably due to oxygen in-leakage through a sediment filter installed in the groundwater pipes just before the heat exchanger. The rest of the systems extract water with similar redox conditions.

The salinity's apparent effect on incrustation type could also be indirect, by its influence on the microbial community. The two most common iron-oxidizing bacteria Gallionella and Leptothrix have been observed to prefer lower salinities (McBeth et al., 2013; Eggerichs et al., 2014). This is in correspondence with the observed iron oxide incrustations and activity of iron-oxidizing bacteria in Melhus, see Fig. 6. The higher loss on ignition (i.e., a proxy for organic matter content) in the low-saline, iron oxide incrusted GWHP systems indicate that bacteria thrive more in these systems.

The GWHP system which has suffered the most clogging issues (i.e., the iron oxide incrusted Lena terrasse (Table 1)) is furthermore

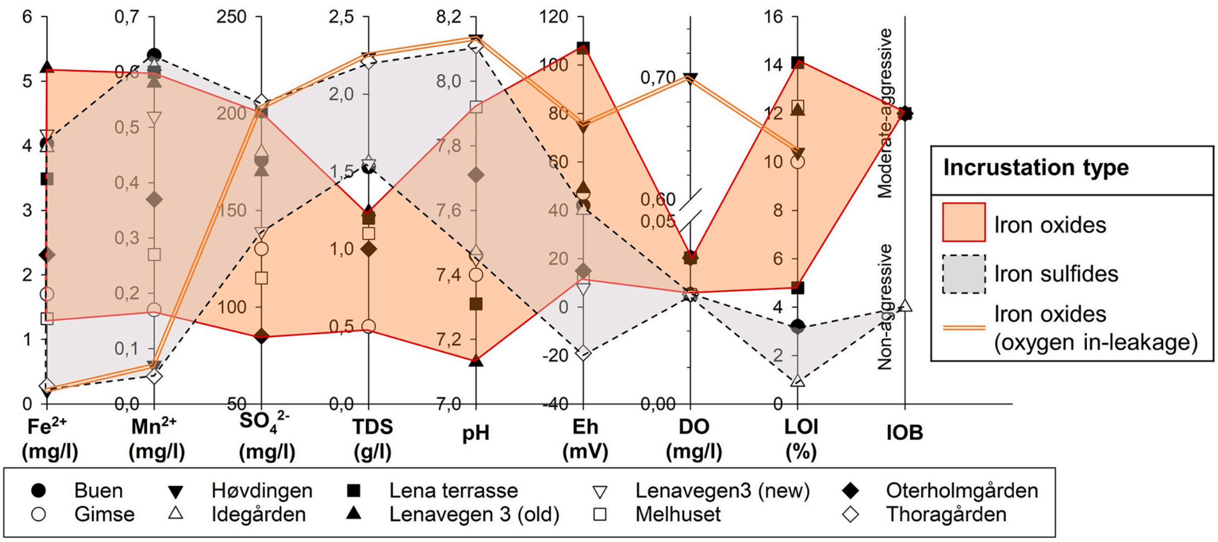

Fig. 6.. Relation between hydrochemistry (average and median values from Table 3) and major chemical incrustation type for groundwater heat pump (GWHP) systems in Melhus, Norway. TDS = total dissolved solids, DO = dissolved oxygen, LOI = loss on ignition, IOB = iron-oxidizing bacteria.

characterized by relatively high iron concentrations (> 3 mg/l) and a circumneutral pH (7.2–7.4), see Fig. 6. These pH conditions are favorable for the neutrophilic (i.e. thrive at circumneutral pH) Gallionella and Leptothrix genera (Eggerichs et al., 2014), while higher iron concentrations at least are favorable for the Gallionella bacteria. The Lena terrasse GWHP also display the highest measured redox potentials (Fig. 6), which indicates that iron oxidation is most active in this system.

From a purely abiotic point of view, a lower pH imposes slower homogenous and heterogenous iron oxidation rates, see Eqs. (2) and (3). Thus, the hydrochemistry of the iron oxide incrusted Oterholmgården and Lena terrasse suggest faster iron oxide clogging at Oterholmgården than Lena terrasse. Using mean/median values from Table 3 inserted in Eqs. (2) and (3), suggest 60–310% faster iron oxidation at Oterholmgården than Lena terrasse, depending on whether homogenous or heterogenous oxidation is rate controlling. This assumes the same rate constants for both systems, due to comparable salinities in the two GWHP systems (Sung and Morgan, 1980). More clogging related rehabilitations and reconstructions (Table 1) and higher redox potentials measured at Lena terrasse than Oterholmgården, rejects the hypothesis of a purely abiotic cause of iron oxide clogging. This further highlights the microbes' importance on iron oxidation and incrustation.

Odor of H_2S gas has been documented in the GWHP systems in Melhus, which together with high ferrous iron concentrations facilitates iron sulfide precipitation. Measured redox potentials (Fig. 6) suggest sulfate reduction is not a governing redox process. This indicates that the iron sulfide formation at Buen, Idegården and Thoragården could be a pure precipitation reaction. Limited sulfate reduction around the well systems also may explain the low sulfate reducing bacteria (SRB) activity deducted from BART tests, see Fig. 2. Possibly, the mechanical incrustations often found together with the iron sulfides (Fig. 5) may be the major clogging process in these well systems.

The hydrochemistry at Lenavegen 3 resembles that of Idegården and Buen, see Fig. 6. Iron sulfides are thus expected to incrust this production well as well. Furthermore, the gravel size (> 2 mm) sediment deposits found in the flow-through cell during measurement at Lenavegen 3 is indicative of serious abrasion/corrosion of the 1 mm production well screen slots. This could possibly have been mediated by incrustations blocking the formation filter and/or well screen.

The magnetism of the incrustation samples from Idegården and Thoragården indicates that these GWHP systems suffer from corrosion. Holes detected in a steel valve in the groundwater pipeline at Idegården in December 2020 further confirms the corrosion problems. The "non-aggressive" SRB activity at Idegården from BART tests is thus surprising, since these bacteria often form essential parts of corrosion processes (Houben and Treskatis, 2007). However, more detailed investigations of the microbiology must be conducted to disprove the presence of SRBs.

The camera inspections show that iron oxides incrust shallower while iron sulfides incrust deeper production wells, see Fig. 5. This corresponds with proximity to the oxic to iron-reducing redox boundary. Still redox species concentrations and measured redox potentials are comparable in the shallow and deep systems. The depth tendency for iron oxide formation also correlates with changing salinity and pH with depth, which could influence microbial activity, as mentioned above.

Some exceptions to the trend of shallow iron oxide and deep iron sulfide incrustations are also found. What resembles iron sulfides have been observed in the bottom part of the relatively long well screens at the Gimse production well (15 m) and the Lena terrasse injection well (10 m). Non-uniform flow through well screens may lead to stagnant zones in the bottom part of the well screens which promotes anoxic conditions (Mansuy, 1998). This could explain the observations at Gimse and Lena terrasse. On the other hand, iron oxides are found in some deep injection wells at Idegården and Høvdingen, which is probably caused by oxygen in-leakage through the surface part of the groundwater pipes. Relatively high oxygen concentrations (> 0.1 mg/l) have been detected in both these GWHP systems, see Table 3. The corrosion holes at Idegården and a leaky sediment filter at Høvdingen are probably responsible for these oxygen levels.

Mechanical incrustations (i.e., sediment deposits) seem to be a bigger problem for injection than production wells. This can be explained by injection wells functioning as a sink for sediments mobilized in the production well. The cementation of mechanical incrustation with iron oxides or sulfides may explain why injection wells suffer more from deteriorating clogging problems. Mobilization in the production well can both be caused by improper well development or filter design, or incrustations blocking the inflow cross-section and causing turbulent flow (Mansuy, 1998; Bakema, 2001). It is noteworthy that the GWHP systems which have suffered the most from mechanical incrustations have (1) relatively short production well filters (3.0–3.5 m) (Buen, Høvdingen, Lenavegen 3, Thoragården) and/or high pumping rates (Lenavegen 3, Lena terrasse), see Table 1. Longer well filter designs and lower pumping rates thus may be a viable measure against mechanical clogging problems in Melhus.

Some uncertainties are associated with the field water quality and the laboratory incrustation analyses. Redox potentials did not stabilize during the two-hour measurement period in any of the GWHP systems. Still, consistent redox levels prevail for each GWHP system over the two-year sampling period. The two-hour reading was thus believed to be indicative of the relative Eh level between the nine GWHP systems. Furthermore, measured oxygen levels are lower than the zero-point of the oxygen sensor. Still, correlations between temperature and oxygen even below the zero-point are observed, which indicates that at least some oxygen is present in the pumped-up groundwater. Lastly, the long storage time of incrustation samples made them vulnerable to oxidation of sulfides and organic matter, and maturation of amorphous iron oxides. Few samples displayed a partition between sulfides and oxides, neither analytically nor visually between core and surface, as would have been expected for partial oxidation of sulfide samples. Organic matter contents (LOI) of iron oxide samples were comparable to those found by McLaughlan (1992) despite long storage periods. This is interpreted as a sign of modest organic matter decomposition with time, and backs up the reliability of the analytical method. The crystallinity of iron oxide incrustation samples detected during XRD analysis were generally low , and thus rule out substantial maturation to have occurred. Consequently, the results and analysis presented here are concluded to be valid.

4.1. Practical implications

Both iron oxides and sulfides incrust the GWHP systems, although most systems extract anoxic water from well below the iron redox boundary. Thus, vertical mixing of water from different redox zones in the production well is probably not triggering the iron oxide precipitation. Furthermore, iron sulfide incrustations are also found. This means locating the production well screen deep beneath the iron redox boundary, as suggested by Possemiers et al. (2016), will probably not prevent incrustation problems in Melhus. The well owners should rather focus on regular maintenance with appropriate rehabilitation methods. Still, this study reveals which conditions are favorable for oxide and sulfide formation, meaning the well designers could to some extent pick their problems from well location and dimensioning.

The range of deteriorating problems detected in the GWHP systems in Melhus justifies proper monitoring and analysis of the incrustation problems. System performance monitoring of pressure, temperature and flow rate, as described in Gjengedal et al. (2020), is a prerequisite for early clogging detection, but does not necessarily provide implications for further actions. This can be illustrated by the difference between iron oxides and sulfides: While iron oxides are best dissolved by the reducing agent sodium dithionite ($Na_2S_2O_4$) under pH neutral conditions (Houben, 2003), this measure will not dissolve iron sulfide incrustations, which are best dissolved by inorganic acids (e.g., hydrochloric acid (HCl) (Houben and Treskatis, 2007)), or an oxidizing agent (e.g., sodium hypochlorite (NaClO) (van Beek and Kooper, 1980)).

Incrustation samples can be hard to obtain but will help to interpret the observations during camera inspections. The GWHP system design should thus facilitate easy access for water and incrustation sampling and camera inspections, as already suggested by Gjengedal et al. (2018). The combination of flow-through cell measurements and BART tests have proven to yield valuable information on biochemical incrustation potential. Both methods are therefore advised to be included for GWHP clogging risk assessment.

5. Conclusions

The investigations presented in this article show that:

- Iron oxides and iron sulfides, together with aquifer sediments, incrust groundwater heat pump (GWHP) systems extracting water from the same saline (total dissolved solids = 0.4–2.4 g/l), anoxic (dissolved oxygen $\leq$ 0.05 mg/l), and iron-rich (dissolved ferrous iron =0.14–6.44 mg/l) aquifer in Melhus.
- Water quality seems to dictate problem type, with sulfides incrusting systems extracting deeper, more saline groundwater, while shallower systems extracting fresher groundwater suffer from iron oxide incrustations. The identification of iron-oxidizing bacteria (IOB) from biological activity reaction tests (BART) solely in iron oxide incrusted GWHP systems, also point to biotic influence on incrustations
- The most frequent clogging problems were detected in the Lena terrasse GWHP system which is clogged by iron oxides and sediments. This GWHP system displays the highest redox potential, high organic matter (LOI) to iron oxide ratios in the incrustations, IOBs present (BART), relatively high groundwater pumping rates and high iron concentrations. This combination of hydrochemical, biotic and hydraulic conditions seems to facilitate severe clogging
- Though type and severity of iron incrustations to some extent could be controlled by location and design of the systems, these clogging issues must be expected in groundwater heat pump systems. Thus, more focus should be directed towards tailored and timed rehabilitations. Detailed water quality and incrustation investigations should be compulsory prior to and during operation to customize cost-effective rehabilitation techniques.

Funding

This work was supported by the Regional Research Funds in Mid-Norway [grant number 284965]; the Norwegian University of Science and Technology (including St. Olav's Hospital - Trondheim University Hospital). The funding sources were not involved in the study design, writing of the report; nor in the decision to submit the article for publication.

Availability of data and material

The authors approve that all data and materials support their published claims and comply with field standards. The authors agree to share their research data.

Ethics approval

The authors approve that they have followed the rules of good scientific practice.

CRediT authorship contribution statement

Lars A. Stenvik: Conceptualization, Data curation, Formal analysis, Investigation, Methodology, Project administration, Software, Visualization, Writing – original draft. **Sondre Gjengedal:** Conceptualization, Data curation, Formal analysis, Investigation, Methodology, Supervision, Visualization, Writing – review & editing. **Randi K. Ramstad:** Conceptualization, Data curation, Formal analysis, Funding acquisition, Investigation, Project administration, Resources, Supervision, Writing – review & editing. **Bjørn S. Frengstad:** Conceptualization, Formal analysis, Funding acquisition, Methodology, Project administration, Resources, Supervision, Validation, Writing – review & editing.

Declaration of Competing Interest

The authors declare that they have no known competing financial interests or personal relationships that could have appeared to influence the work reported in this paper.

Acknowledgements

This study is part of the research project Optimal Utilization of Groundwater for Heating and Cooling in Melhus 2 (ORMEL 2). This is a cooperation between Melhus municipality, the Norwegian University of

Science and Technology, Asplan Viak AS, the Geological Survey of Norway and Gjøvaag AS, receiving funding from the Regional Research Funds in Mid-Norway. We would like to thank all the involved institutions and persons for cooperation and financial support, and all the helpful janitors at the GWHP plants in Melhus. We would also like to thank senior engineers Torill Sørløkk and Laurentius Tijhuis at the mineralogical lab for help with XRD, ICP-MS and LOI analysis and discussions, and to staff engineer Håkon Myhren at the mechanical lab who designed, built, and rehabilitated the flow-through cell (all three at the Department of Geoscience and Petroleum, NTNU). Furthermore, many thanks to Dr. Georg J. Houben at the Federal Institute for Geosciences and Natural Resources (BGR) in Hannover, Germany for helpful input on iron bacteria, and to Dr. Clara Sena at the University of Oslo for discussions and input on data interpretation and presentation. Finally, the authors would like to thank the two reviewers for their constructive comments and feedback.

Supplementary materials

Supplementary material associated with this article can be found, in the online version, at doi:10.1016/j.geothermics.2022.102349.

References

Bakema, G., 2001. Well and Borehole Failures and Solutions in Underground Thermal Energy Storage. IF Technology, Arnhem. https://doi.org/10.13140/RG.2.2.10214.98885. IF Technology report 2/9805/GW.

Barbič, F.F., Bracilovič, D.M., Djindjič, M.V., Djorelijevski, S.M., Ẑivkovič, J.S., Krajinčanič, B.V., 1974. Iron and manganese bacteria in Ranney wells. Water Res. 8 (11), 895–898. https://doi.org/10.1016/0043-1354(74)90103-1.

Brøste, H.M., 2017. Vannkvalitet Knyttet til Grunnvannsbaserte grunnvarmeanlegg i Melhus og Elverum [Eng: Water Quality in Groundwater-Based Heat Pump Systems in Melhus and Elverum. NTNU, Trondheim. In Norwegian] (Master thesis).

Burté, L., Cravotta III, C.A., Bethencourt, L., Farasin, J., Pédrot, M., Dufresne, A., Gerard, M.F., Baranger, C., Le Borgne, T., Aquilina, L, 2019. Kinetic study on clogging of a geothermal pumping well triggered by mixing-induced biogeochemical reactions. Environ. Sci. Technol. 53 (10), 5848–5857. https://doi.org/10.1021/acs.est.9b00453.

Cullimore, D.R., 2008. Practical Manual of Groundwater Microbiology, 2nd ed. CRC Press, Boca Raton.

Dimkić, M., Pušić, M., Obradović, V., Kovačević, S., 2012. The effect of certain biochemical factors on well clogging under suboxic and mildly anoxic conditions. Water Science and Technology 65 (12), 2206–2212. https://doi.org/10.2166/wst.2012.129.

Eggen, G., Vangsnes, G., 2005. Heat pump for district cooling and heating at Oslo airport, Gardermoen. In: Axell, M. (Ed.), 8th IEA Heat Pump Conference. Las Vegas, USA. Borås, Ed. IEA Heat Pump Centre.

Eggerichs, T., Opel, O., Otte, T., Ruck, W., 2014. Interdependencies between biotic and abiotic ferrous iron oxidation and influence of pH, Oxygen and Ferric Iron Deposits. Geomicrobiol. J. 31 (6), 461–472. https://doi.org/10.1080/01490451.2013.870620.

Gjengedal, S., Ramstad, R.K., Hilmo, B.O., Frengstad, B.S., 2018. Video inspection of wells in open loop ground source heat pump systems in Norway. IGSHPA Research Track, Stockholm. Oklahoma State University, Sweden. Stillwater. https://doi.org/10.22488/okstate.18.000025.

Gjengedal, S., Stenvik, L.A., Storli, P.T.S., Ramstad, R.K., Hilmo, B.O., Frengstad, B.S., 2019. Design of Groundwater Heat Pump Systems. Principles, Tools, and Strategies for Controlling Gas and Precipitation Problems. Energies 12 (19), 3657. https://doi.org/10.3390/en12193657.

Gjengedal, S., Ramstad, R.K., Hilmo, B.O., Frengstad, B.S., 2020. Fouling and clogging surveillance in open loop GSHP systems. Bull. Eng. Geol. Environ. 79, 69–82. https://doi.org/10.1007/s10064-019-01556-5.

Hellestveit, M.S., 2018. 3D-Modellering av Grunnvannstrømning og Varmetransport i Akviferen i Melhus sentrum [Eng: 3D Modelling of Groundwater Flow and Heat Transport in the Aquifer in Central Melhus. NTNU, Trondheim. In Norwegian] (Master thesis).

Houben, G.J., 2003. Iron oxide incrustations in wells. Part 2: chemical dissolution and modeling. Appl. Geochem. 18 (6), 941–954. https://doi.org/10.1016/S0883-2927(02)00185-3.

Houben, G.J., 2004. Modeling the Buildup of Iron Oxide Encrustations in Wells. Groundwater 42 (1), 78–82. https://doi.org/10.1111/j.1745-6584.2004.tb02452.x.

Houben, G.J., Treskatis, C., 2007. Water Well Rehabilitation and Reconstruction. McGraw-Hill, New York.

Lerm, S., Alawi, M., Miethling-Graff, R., Wolfgramm, M., Rauppach, K., Seibt, A., Würdemann, H., 2011. Influence of microbial processes on the operation of a cold store in a shallow aquifer: impact on well injectivity and filter lifetime. Grundwasser 16 (2), 93–104. https://doi.org/10.1007/s00767-011-0165-x.

Mansuy, N., 1998. Water Well rehabilitation: A practical Guide to Understanding Well Problems and Solutions. CRC Press, Boca Raton.

McBeth, J.M., Fleming, E.J., Emerson, D., 2013. The transition from freshwater to marine iron-oxidizing bacterial lineages along a salinity gradient on the Sheepscot River. Environ. Microbiol. Rep. 5 (3), 453–463. https://doi.org/10.1111/1758-2229.12033.

McLaughlan, R.G., 1992. Fouling and Corrosion of Groundwater Wells in Australia. University of New South Wales, Kensington. Ph.D. thesis.

Possemiers, M., Huysmans, M., Anibas, C., Batelaan, O., Van Steenwinkel, J., 2016. Reactive transport modeling of redox processes to assess Fe(OH)3 precipitation around aquifer thermal energy storage wells in phreatic aquifers. Environ. Earth Sci. 75, 648. https://doi.org/10.1007/s12665-016-5398-7.

Reite, A.J., 1990. Sør-Trøndelag fylke: Kvartærgeologisk Kart M 1:250.000: Veiledning Til Kartet [Eng: Sør-Trøndelag county: Quaternary geology Map M 1:250.000 : Guidance to the map. In Norwegian]. Skrifter 96. Geological Survey of Norway, Trondheim.

Riise, M.H., 2015. Praktisk guide for grunnvarmeanlegg basert på oppumpet grunnvann: Hydrogeologiske forundersøkelser, etablering, Drift og oppfølging med utgangspunkt i erfaringer fra etablerte anlegg i Melhus sentrum [Eng: Practical Guide for Ground Water Heat Pump Systems. NTNU, Trondheim. In Norwegian(Master thesis.

Solberg, I.L., Dagestad, A., Dalsegg, E., 2014. 2D resistivitetsmålinger ved Brubakken, Melhus sentrum og Skjerdingstad i Melhus kommun, Sø-Trønderlag. Data og tolkninger [Eng: 2D resistivity measurements at Brubakken, Melhus town center and Skjerdingstad in Melhus municipality. Data and interpretations. Geological Survey of Norway, Trondheim. In NorwegianNGU report 2014.022.

Statistics Norway. (2020). Population and land area in urban settlements. https://www.ssb.no/en/befolkning/folketall/statistikk/tettsteders-befolkning-og-areal. Accessed 30 August 2021.

Stumm, W., Lee, G.F., 1961. Oxygenation of Ferrous Iron. Ind. Eng. Chem. 53 (2), 143–146. https://doi.org/10.1021/ie50614a030.

Stumm, W., Morgan, J.J., 1996. Aquatic chemistry: Chemical Equilibria and Rates in Natural Waters, 3rd ed. John Wiley & Sons Inc, Hoboken.

Sung, W., Morgan, J.J., 1980. Kinetics and product of ferrous iron oxygenation in aqueous systems. Environ. Sci. Technol. 14 (5), 561–568. https://doi.org/10.1021/es60165a006.

Tamura, H., Goto, K., Nagayama, M., 1976. The effect of ferric hydroxide on the oxygenation of ferrous ions in neutral solutions. Corrosion Sci. 16 (4), 197–207. https://doi.org/10.1016/0010-938X(76)90046-9.

van Beek, C.G.E.M., 1989. Rehabilitation of clogged discharge wells in the Netherlands. Q. J. Eng. Geol. Hydrogeol. 22, 75–80. https://doi.org/10.1144/GSL.QJEG.1989.022.01.06.

van Beek, C.G.E.M., Kooper, W.F., 1980. The clogging of shallow discharge wells in the Netherlands river region. Groundwater 18 (6), 578–586. https://doi.org/10.1111/j.1745-6584.1980.tb03652.x -0537-9.